

**NASA Technical Memorandum 104599**

**MODIS Airborne Simulator Visible  
and Near-Infrared Calibration -  
1992 ASTEX Field Experiment**

*Calibration Version - ASTEX King 1.0*

**G. Thomas Arnold**  
*Applied Research Corporation*  
*Landover, Maryland*

**Michael Fitzgerald**  
**Patrick S. Grant**  
*ATAC*  
*Mountain View, California*

**Michael D. King**  
*Goddard Space Flight Center*  
*Greenbelt, Maryland*



National Aeronautics and  
Space Administration

**Goddard Space Flight Center**  
Greenbelt, Maryland

1994



## Table of Contents

<u>Section</u>	<u>Page</u>
I. Introduction.....	1
II. Hemisphere Calibration .....	1
III. MAS Calibration Procedure and Data .....	1
IV. Temperature Sensitivity of MAS Calibration.....	10
V. Intercomparison of Field Calibration to Ames 30-Inch Sphere Calibration.....	13
VI. Future Calibration Work.....	19



## **I. Introduction**

Calibration of the visible and near-infrared (near-IR) channels of the MODIS Airborne Simulator (MAS) is derived from observations of a calibrated light source. For the 1992 Atlantic Stratocumulus Transition Experiment (ASTEX) field deployment, the calibrated light source was the NASA Goddard 48-inch integrating hemisphere. Tests during the ASTEX deployment were conducted to calibrate the hemisphere and then the MAS. This report summarizes the ASTEX hemisphere calibration, and then describes how the MAS was calibrated from the hemisphere data. All MAS calibration measurements are presented and determination of the MAS calibration coefficients (raw counts to radiance conversion) is discussed. In addition comparisons to an independent MAS calibration by Ames personnel using their 30-inch integrating sphere is discussed.

## **II. Hemisphere Calibration**

During the ASTEX deployment several calibrations of the Goddard 48-inch hemisphere were conducted. To calibrate the hemisphere, the hemisphere was operated at full intensity (all 12 lamps on) and the sphere output was measured at regular intervals over a broad wavelength range using an Optronic 746 Monochromater. For measurements in the visible wavelength region a silicon detector with a grating blazed at 0.75  $\mu\text{m}$  was used, and for the longer near-IR wavelengths a lead sulfide detector with a grating blazed at 2.5  $\mu\text{m}$  was used (the cooled germanium detector with a grating blazed at 1.6  $\mu\text{m}$  proved unreliable for this deployment). These measurements were then calibrated from observations of a single standard lamp using the same monochromater. Table 1 below summarizes the ASTEX monochromater data (as converted to radiance from the standard lamp observations). The column labeled Pre-ASTEX is the results of the hemisphere calibration conducted just before shipping the hemisphere to the Azores (this is a benchmark to note significant changes in the hemisphere data due to shipping). In the ASTEX Avg. column are the average radiance for each wavelength for all hemisphere calibrations conducted during the mission. In the last column are the standard deviation values for each ASTEX Avg. radiance. Note that for ASTEX data, the hemisphere radiance for 0.85 - 1.1  $\mu\text{m}$  have been normalized using a Planck interpolation method. This was necessary due to problems incurred measuring the data at these wavelengths. Figure 1 comparing the radiance values before and after the Planck correction clearly shows a more realistic curve with the correction added.

In addition to calibrating the hemisphere at full intensity, tests were conducted to determine the radiance (at a particular wavelength) at less than full intensity. Starting with all 12 lamps on, lamps were turned off one at a time and the corresponding relative change in intensity noted. This test was repeated at 0.05  $\mu\text{m}$  intervals from 0.4-0.95  $\mu\text{m}$  and then all the relative intensities for each lamp level were averaged. The average relative intensity values for ASTEX are shown in Table 2. Due to the small (typically less than one percent) variation in the relative intensities for various wavelengths, the individual relative intensity values are considered independent of wavelength.

## **III. MAS Calibration Procedure and Data**

Calibration of the MAS visible and near-IR channels is accomplished by observing different output intensities of the 48-inch hemisphere and correlating the observed MAS 'counts' values to the known hemisphere radiance values. For ASTEX the calibration tests were conducted on three different days inside the ER-2 hangar in Lajes. To conduct the calibration it was necessary to remove the instrument from the ER-2 wing pod and set it up on a stand directly in front of the 10 inch vertical opening in the flat side of the hemisphere. Then a front surface mirror was placed directly below the scan mirror, angled at 45° to both MAS nadir and the horizontal output beam of the hemisphere. Use of this mirror naturally degrades the observed radiance, and thus the spectral reflection of the mirror has been charac-

terized. The results of this characterization and its effect on each MAS channel are presented in Table 3.

Table 1. Hemisphere Radiance for 48-inch Hemisphere Before and During ASTEX Mission, and the Standard Deviation of the ASTEX Measurements.

Wavelength ( $\mu\text{m}$ )	Pre-ASTEX $\text{mW}/(\text{cm}^2\text{-}\mu\text{m}\text{-sr})$	ASTEX Avg $\text{mW}/(\text{cm}^2\text{-}\mu\text{m}\text{-sr})$	Std. Dev. of ASTEX (Avg. in %)
0.60	12.17	12.22	2.29
0.65	15.07	15.06	2.36
0.70	17.57	17.52	2.09
0.75	19.49	19.25	2.02
0.80	20.95	20.58	1.99
0.85	21.73	21.25*	2.10
0.90	22.04	21.40*	2.13
0.95	22.27	20.66*	1.64
1.00	22.07	20.64*	1.61
1.05	21.59	21.21*	1.82
1.10	20.48	19.56	3.11
1.15	19.49	18.43	2.57
1.20	18.53	16.39	2.09
1.25	17.65	16.72	1.77
1.30	16.45	15.56	1.68
1.35	14.94	13.99	1.67
1.40	13.08	12.65	4.13
1.45	12.25	11.47	3.31
1.50	11.82	11.50	3.32
1.55	10.93	10.73	4.25
1.60	10.52	10.15	1.49
1.65	10.14	9.50	1.55
1.70	8.85	8.64	2.37
1.75	8.18	7.86	1.05
1.80	7.34	7.05	2.04
1.85	6.70	6.33	1.76
1.90	4.95	5.04	4.68
1.95	4.65	4.70	4.33
2.00	4.72	4.72	2.98
2.05	4.68	4.32	4.46
2.10	4.09	4.02	4.74
2.15	3.74	3.83	7.35

Note: The \* denotes normalized Planck interpolated data

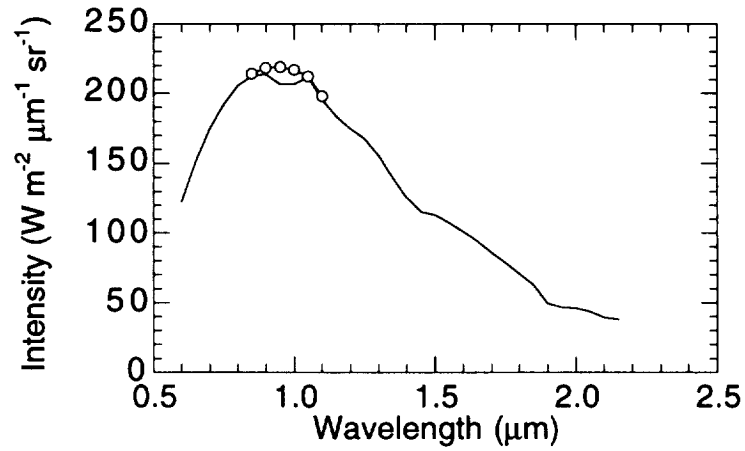


Figure 1. Plot of average hemisphere intensity (ASTEX Avg column in Table 1) vs. wavelength. Also shown is the Planck correction that was applied to the data due to instrument measurement errors in the 0.85 to 1.1 μm range.

Table 2. Average Relative Intensity for Each Hemisphere Lamp for all Measurements Between 0.4 and 0.95 μm

No. of Lamps Turned On	Relative Intensity
12	1.000
11	0.907
10	0.833
9	0.753
8	0.656
7	0.578
6	0.501
5	0.413
4	0.323
3	0.246
2	0.165
1	0.083

**Table 3. Characterization of the Front Surface Mirror Used in MAS Calibration and Interpolation of Reflectance Values to MAS Wavelengths**

Wavelength ( $\mu\text{m}$ )	Average Reflectance (%)	MAS wavelength ( $\mu\text{m}$ )	Reflectance (%)
0.60	89.68		
0.65	86.24	0.665	85.40
0.70	83.45		
0.75	79.48		
0.80	75.38		
0.85	72.98	0.875	75.89
0.90	78.81	0.945	83.09
0.95	83.57		
1.00	87.85		
1.05	90.35		
1.10	91.37		
1.15	92.57		
1.20	93.49		
1.25	94.19		
1.30	94.64		
1.35	94.98		
1.40	95.51		
1.45	95.78		
1.50	96.39		
1.55	95.92		
1.60	96.75	1.6230	97.19
1.65	97.70		
1.70	96.59		
1.75	98.89		
1.80	98.24		
1.85	99.01		
1.90	97.69		
1.95	96.73		
2.00	99.37		
2.05	96.20		
2.10	96.20	2.1420	97.28
2.15	97.48		

With the MAS carefully aligned with the hemisphere radiance, starting at full intensity (12 lamps), then turning off pairs of lamps, observations of each hemisphere radiance level were recorded. Table 4 (a-e) summarizes by channel all the MAS calibration measurements taken during ASTEX. Note that channels 2-6 are all recorded at 8 bits and thus all counts values in Table 4 are between 0 and 255.

Since MAS counts values are by design linearly proportional to radiance, a radiance per count factor for each channel can be determined by a simple linear regression of the MAS counts for each channel and the associated hemisphere radiance values. Thus appropriate hemisphere radiance values must be determined for each of MAS channels 2-6. One method is to determine the hemisphere radiance at the wavelength of the peak power point of the spectral response curve for each channel's bandpass filter function. Then interpolate from the values in Table 1 the appropriate hemisphere radiance. A second method is to interpolate the hemisphere data for the wavelength region of the bandpass filter for each channel and then integrate over the entire bandpass filter. Generally the second method is preferable, however for the ASTEX data, the first method has been chosen. Using the interpolated radiance at the filter's peak power point is considered adequate for this data due to the

relatively narrow MAS bandwidths (equal to or only slightly greater than the 0.05 $\mu\text{m}$  sampling interval for the hemisphere data), and as will be shown in the final section of this report, the differences in the two methods of radiance determination are about a percent or less and thus are smaller than the standard deviation values of the hemisphere calibration.

The result of each linear regression of MAS counts and their associated radiance values is a radiance per count factor (slope) and a radiance offset (intercept). The radiance per count and radiance offset values for the 9 tests are given in Tables 5 (a-e). Generally the results show good agreement in tests 1, 2, 3, 4, 7, 8, and 9. The notable exception is tests 1 and 2 for channel 2. These two tests differ from the others since after they were conducted, a resistor in the MAS was changed to eliminate a 'clipping' problem in the data (data saturating at a value less than 255 counts). Adding the resistor resulted in about a 20% decrease in the gain. Thus calibration data for ASTEX flights previous to this resistor change will be based on calibration tests 1 and 2.

Table 4 (a-e). Summary of All MAS Hemisphere Observations for ASTEX

(a)  
Channel 2 - 0.665  $\mu\text{m}$

No. of lamps	Test 1	Test 2	Test 3	Test 4	Test 5	Test 6	Test 7	Test 8	Test 9
12	50	202	82	83	76	155		82	82
10	42	172	70	71	65	132	140	70	70
8	34	139	57	57	53	108	114	57	57
6	27	110	46	46	43	87	91	46	46
4	19	78	33	33	31	63	66	33	33
2	12	50	22	22	21	43	44	22	22
0	5	21	10	10	10	20	21	10	10
gain	1	4	2	2	2	4	4	2	2

(b)  
Channel 3 - 0.875  $\mu\text{m}$

No. of lamps	Test 1	Test 2	Test 3	Test 4	Test 5	Test 6	Test 7	Test 8	Test 9
12	73	146	73	83	68	155		72	72
10	61	123	61	71	57	132	61	61	61
8	49	94	49	57	46	108	49	49	49
6	38	76	38	46	35	87	38	38	38
4	26	53	26	33	24	63	26	26	26
2	15	31	15	22	15	43	15	15	15
0	4	9	4	10	4	20	4	4	4
gain	1	2	1	1	2	4	1	1	1

(c)  
Channel 4 - 0.945  $\mu\text{m}$

No. of lamps	Test 1	Test 2	Test 3	Test 4	Test 5	Test 6	Test 7	Test 8	Test 9
12								252	252
10	230	230	230	230	213	107	226	227	226
8	182	182	182	182	169	85	179	179	179
6	138	138	138	138	128	64	135	135	135
4	91	91	91	91	85	42	89	90	89
2	48	48	48	48	45	22	48	48	48
0	4	4	4	4	4	2	4	4	4
gain	1	1	1	1	1	0.5	1	1	1

(d)  
Channel 5 - 1.623  $\mu\text{m}$

No. of lamps	Test 1	Test 2	Test 3	Test 4	Test 5	Test 6	Test 7	Test 8	Test 9
12		189				155			
10		158			249	130	160		
8	252	126	253		200	105	127		
6	191	96	192	193	152	80	97	198	199
4	129	65	130	131	103	54	65	133	134
2	71	35	71	71	58	30	36	73	73
0	11	5	11	11	10	5	5	11	10
gain	2	1	2	2	2	1	1	2	2

(e)  
Channel 6 - 2.142  $\mu\text{m}$

No. of lamps	Test 1	Test 2	Test 3	Test 4	Test 5	Test 6	Test 7	Test 8	Test 9
12		180			195	99			
10		151			166	84	153		
8	242	122	242	244	135	68	123	250	252
6	185	93	185	186	105	53	94	191	192
4	127	64	128	129	75	38	65	132	132
2	73	36	73	73	46	23	37	75	75
0	16	8	16	17	16	8	8	16	16
gain	4	2	4	4	4	2	2	4	2

Table 5. MAS Calibration Coefficients for Each Visible and Near-IR Channel and the Dates They Were Determined

(a)  
Channel 2 - 0.665  $\mu\text{m}$

Test No.	Date	Correlation Coefficient	Rad/Count* (Slope)	Radiance offset† (Intercept)
1	6/15/92	0.99988	3.000E+00	-1.394E+00
2	6/15/92	0.99997	2.962E+00	-1.450E+00
3	6/15/92	0.99999	3.752E+00	-1.867E+00
4	6/15/92	0.99988	3.695E+00	-1.792E+00
5	6/24/92	0.99998	4.092E+00	-2.033E+00
6	6/24/92	0.99995	4.014E+00	-2.009E+00
7	6/26/92	1.00000	3.752E+00	-1.841E+00
8	6/26/92	0.99999	3.752E+00	-1.867E+00
9	6/26/92	0.99999	3.752E+00	-1.867E+00

(b)  
Channel 3 - 0.875  $\mu\text{m}$

Test No.	Date	Correlation Coefficient	Rad/Count* (Slope)	Radiance offset† (Intercept)
1	6/15/92	0.99996	2.381E+00	-8.883E-01
2	6/15/92	0.99940	2.396E+00	-9.294E-01
3	6/15/92	0.99996	2.381E+00	-8.883E-01
4	6/15/92	0.99996	2.381E+00	-8.883E-01
5	6/24/92	0.99977	2.571E+00	-9.886E-01
6	6/24/92	0.99995	2.547E+00	-1.047E+00
7	6/26/92	1.00000	2.397E+00	-9.388E-01
8	6/26/92	0.99997	2.403E+00	-9.397E-01
9	6/26/92	0.99997	2.403E+00	-9.397E-01

(c)  
Channel 4 - 0.945  $\mu\text{m}$

Test No.	Date	Correlation Coefficient	Rad/Count* (Slope)	Radiance offset† (Intercept)
1	6/15/92	0.99996	6.703E-01	-2.259E-01
2	6/15/92	0.99996	6.703E-01	-2.259E-01
3	6/15/92	0.99996	6.703E-01	-2.259E-01
4	6/15/92	0.99996	6.703E-01	-2.259E-01
5	6/24/92	0.99954	7.250E-01	-2.652E-01
6	6/24/92	0.99939	7.190E-01	-2.007E-01
7	6/26/92	0.99990	6.822E-01	-2.179E-01
8	6/26/92	0.99990	6.815E-01	-2.411E-01
9	6/26/92	0.99992	6.838E-01	-2.554E-01

Table 5 (cont'd). MAS Calibration Coefficients for Each Visible and Near-IR Channel and the Dates They Were Determined

(d)  
Channel 5 - 1.623  $\mu\text{m}$

Test No.	Date	Correlation Coefficient	Rad/Count* (Slope)	Radiance offset† (Intercept)
1	6/15/92	0.99986	5.195E-01	-2.602E-01
2	6/15/92	0.99996	5.175E-01	-2.523E-01
3	6/15/92	0.99987	5.169E-01	-2.591E-01
4	6/15/92	0.99984	5.194E-01	-2.754E-01
5	6/24/92	0.99992	6.631E-01	-3.341E-01
6	6/24/92	0.99994	6.341E-01	-3.336E-01
7	6/26/92	1.00000	5.119E-01	-2.440E-01
8	6/26/92	0.99994	5.069E-01	-2.693E-01
9	6/26/92	0.99992	5.037E-01	-2.652E-01

(e)  
Channel 6 - 2.142  $\mu\text{m}$

Test No.	Date	Correlation Coefficient	Rad/Count* (Slope)	Radiance offset† (Intercept)
1	6/15/92	0.99986	4.360E-01	-1.744E-01
2	6/15/92	0.99993	4.332E-01	-1.705E-01
3	6/15/92	0.99986	4.360E-01	-1.744E-01
4	6/15/92	0.99979	4.321E-01	-1.729E-01
5	6/24/92	0.99993	8.323E-01	-3.404E-01
6	6/24/92	0.99994	8.195E-01	-3.302E-01
7	6/26/92	0.99990	4.285E-01	-1.726E-01
8	6/26/92	0.99984	4.210E-01	-1.706E-01
9	6/26/92	0.99991	4.203E-01	-1.704E-01

\* Radiance/count values have units of  $\text{W m}^{-2} \mu\text{m}^{-1} \text{sr}^{-1} \text{cnt}^{-1}$

† Radiance offset values have units of  $\text{W m}^{-2} \mu\text{m}^{-1} \text{sr}^{-1}$ .

Note in Table 5 that the radiance/count values for channels 5 and 6 for tests 5 and 6 are notably higher than for any of the other tests. Environmental conditions for these two tests however were much different than for the others. The humidity on 6/24 was quite high and no attempt was made during the calibration to reduce it (as on 6/26, tests 7-9). More recent experience with the MAS calibration has shown that 20-30 minutes is needed for the instrument to return completely to nominal counts after filling the dewars with LN2 in moderately humid conditions. The effect is observed to be related to the humidity level. It is presumed that the LN2 vapors cool the dewar window and focusing lenses to below the dew point. (Dew is often observed after filling). Thus unintentional fogging of the optics occurs initially but then begins to dry out as the ambient temperature rises due to the heat generated by both the instrument and the integrating hemisphere. Consistent with this principle are the slightly smaller radiance/count values in test 6 as compared to test 5 (test 6 was conducted less than 30 minutes after test 5). This effect (even more pronounced) was also noted in MAS FIRE-Cirrus calibration when calibrating under high humidity conditions. Therefore sufficient evidence exists to justify not using the data for tests 5 and 6 in determining the final calibration coefficients. Furthermore note that specific plans to incorporate better temperature stability, LN2 venting, and humidity reduction will be instituted for all calibrations beginning in the spring of 1994 to alleviate such future problems. Also relative calibrations (soon to be absolute calibrations) are now taken prior to every flight. This allows for a statistical approach to be taken and bad data to be investigated and thrown out if necessary.

To determine the actual calibration coefficients to apply to the ASTEX data, an average of all the tests (except for the high humidity calibration data of tests 5 and 6) has been calculated. Note however due to necessary changes that occurred during the ASTEX mission in the calibrations of channels 2 and 3, it is not possible to give just a single set of calibration coefficients valid for the entire mission. Thus four different tables are given in Table 6 (a-d). On 6/3/92 the gain in channel 2 was cut by a factor of four to help eliminate a 'clipping' error. Thus in Table 6 (b), the radiance/count for channel 2 increases by a factor of 4 from that in Table 6 (a). (The factor of 4 change is estimated from the factory specifications for type of resistor installed into the MAS. However past calibration checks have shown that the real gain change produced by adding new resistors is within a few percent of what the factory specifications suggest.) In Table 6 (c), due to a resistor change in channel 3 on 6/7/92, the radiance/count value is higher than in (b) by a factor of 2 (also estimated from the resistor's factory specifications). In Table 6 (d) channel 2 gain has been cut (by about an additional 20%). All Table 6 data for channels 4, 5, and 6 is the same.

Also note in Table 6 that the intercept values have not been included. These data are not necessary for final calibration because in-flight the MAS references a cold internal blackbody as a visible zero target. The number of counts each of the visible and near-IR channels 'sees' when observing the blackbody is considered zero radiance. These counts at zero radiance are the system offset and are independent of the magnitude of the radiance/count values. Thus to properly calibrate an earth-view counts value this offset must be first subtracted from the earth-view count. The offset corrected earth-view count is then multiplied by the radiance/count factor in Table 6 below. (Note these offset values are always recorded at a gain of 1.0 and must therefore be multiplied by the gain switch setting before being subtracted from the earth-view counts.)

Table 6. Final Radiance/Count (Slope) Values for ASTEX, Valid for Gain Setting of 1.0

(a)

Counts to radiance conversion for data collected May 31 - June 3, 1992		
Channel	Wavelength ( $\mu\text{m}$ )	Radiance/Count $\text{W m}^{-2} \mu\text{m}^{-1} \text{sr}^{-1} \text{cnt}^{-1}$
2	0.665	7.453E-01
3	0.875	1.196E+00
4	0.945	6.755E-01
5	1.623	5.137E-01
6	2.142	4.296E-01

(b)

Counts to radiance conversion for data collected June 04-06, 1992		
Channel	Wavelength ( $\mu\text{m}$ )	Radiance/Count $\text{W m}^{-2} \mu\text{m}^{-1} \text{sr}^{-1} \text{cnt}^{-1}$
2	0.665	2.981E+00
3	0.875	1.196E+00
4	0.945	6.755E-01
5	1.623	5.137E-01
6	2.142	4.296E-01

Table 6. (con't) Final Radiance/Count (Slope) Values for ASTEX, Valid for Gain Setting of 1.0

(c)

Counts to radiance conversion for data collected June 8-14, 1992		
Channel	Wavelength ( $\mu\text{m}$ )	Radiance/Count $\text{W m}^{-2} \mu\text{m}^{-1} \text{sr}^{-1} \text{cnt}^{-1}$
2	0.665	2.981E+00
3	0.875	2.392E+00
4	0.945	6.755E-01
5	1.623	5.137E-01
6	2.142	4.296E-01

(d)

Counts to radiance conversion for data collected June 15-30, 1992		
Channel	Wavelength ( $\mu\text{m}$ )	Radiance/Count $\text{W m}^{-2} \mu\text{m}^{-1} \text{sr}^{-1} \text{cnt}^{-1}$
2	0.665	3.741E+00
3	0.875	2.392E+00
4	0.945	6.755E-01
5	1.623	5.137E-01
6	2.142	4.296E-01

Note: Divide radiance/count values in above tables by the in-flight gain setting to derive the actual value to apply to the raw data counts.

#### IV. Temperature Sensitivity of MAS Calibration

During ASTEX flights the MAS cooled to near  $-15^{\circ}\text{C}$  (significantly colder than the typical  $+25^{\circ}\text{C}$  laboratory calibration environment). However due to a design problem in the port 2 dewar (housing the near-IR detectors), the calibration of the near-IR channels changes as the instrument cools in-flight. The problem with this early dewar design was that the detectors were mounted by a stem to the top of the dewar, causing the detectors to follow the movement of the outer case of the dewar. Thus the detectors tend to shift out of the beam as the dewar outer case is cooled (by the cold ambient air temperatures). Previous to FIRE-Cirrus there was no time available to address this problem. Between the FIRE-Cirrus and ASTEX deployments time allowed only a temporary solution of adding heater jackets to the dewar to partially heat the dewar, significantly reducing the problem though not eliminating it. New dewars scheduled for installation in the spring of 1994 will eliminate this problem.

To characterize the sensitivity of the calibration of the port 2 near-IR channels to instrument temperature for ASTEX data, calibration tests were conducted inside a cold chamber at Ames both before and after deployment. In the cold chamber the MAS observed a 'constant source' light box. First at room temperature (and atmospheric pressure) the light box radiance was measured. Then the chamber was cooled to  $-35^{\circ}\text{C}$ , allowed to stabilize and the light box was again observed and the measurements recorded. The results are given in Table 7. Note the port 1 channels (2-4) show negligible change with temperature. However the port 2 channels (5 and 6) show (averaging the Pre and Post-ASTEX data) a roughly 15 and 14% change respectively. Note that while this is still significant, the 15 and 14 % values are reduced appreciably from the 33 and 42% values noted in the post-FIRE-Cirrus cold chamber test. The improvement is attributed directly to the addition of the heater jackets on the port 2 dewar prior to the ASTEX deployment.

Table 7. Summary of Pre- and Post-ASTEX Cold Chamber Data Tests, Temperatures are in °C and Channel Values and Offsets are in Raw Counts

Pre-ASTEX Cold Chamber Data					
Temperature	Channel 2	Channel 3	Channel 4	Channel 5	Channel 6
25	241	182	166	172	188
-35	233	178	166	144	161
offsets	40	16	8	11	16
gain settings	8	4	2	2	4
% change	4.0	2.4	0.0	17.4	15.7

Post-ASTEX Cold Chamber Data					
Temperature	Channel 2	Channel 3	Channel 4	Channel 5	Channel 6
25	79	183	160	166	183
-35	78	181	159	147	164
offsets	41.6	18	8	11	16
gain settings	8	4	2	2	4
% change	2.7	1.2	0.7	12.3	11.4

Note: The gain settings apply to all count values in the table. Offset values are subtracted from each channel value before computing % change from +25 to -35°C.

Due to the temperature sensitivity of MAS channels 5 and 6 indicated in Table 7, the laboratory calibration values in Table 6 are not directly applicable to in-flight earth-view counts data. To enable such usage of the laboratory coefficients, an adjustment to the in-flight earth-view counts is necessary to correct for this temperature sensitivity. However before quantitatively defining this adjustment, the instrument temperature (upon which the adjustment is dependent) must first be defined. Determination of instrument temperature ( $T_{mas}$ ) is complicated by different cooling rates of different instrument components due to their degree of exposure to the cold environment, mass, and position relative to heated components of the instrument. To monitor the temperature a Rustrak recording system with four different thermistors was used. MAS engineers suggest use of the thermistor on the optics housing to be the best method of determining the 'true' instrument temperature. For ASTEX the Rustrak data were recorded on flights 92-102 through 92-106 (02 June - 12 June) and is shown in Figure 2. Analysis of these data and similar Rustrak temperature data for the 1991 FIRE-Cirrus mission and TOGA/COARE shows that  $T_{mas}$  can be adequately described by an average of all these curves (for ASTEX data deviation from the average is typically less than  $\pm 2$  °C which translates to less than 1% error in the final calibration). Figure 3 shows the resulting average curve for the ASTEX data. Using a polynomial curve-fit technique, the equation below defines  $T_{mas}$  for all ASTEX flights:

$$T_{mas} = M_0 + M_1 * T_{dh} + M_2 * (T_{dh})^2 + M_3 * (T_{dh})^3 + M_4 * (T_{dh})^4 + M_5 * (T_{dh})^5, \text{ where } (1)$$

$T_{dh}$  is the time (in decimal hours) from takeoff  
 $M_0 = 2.4139E+01$   
 $M_1 = -3.0864E+01$   
 $M_2 = 1.1150E+01$   
 $M_3 = 2.0691E+00$   
 $M_4 = 1.9371E-01$   
 $M_5 = -7.2359E-03$

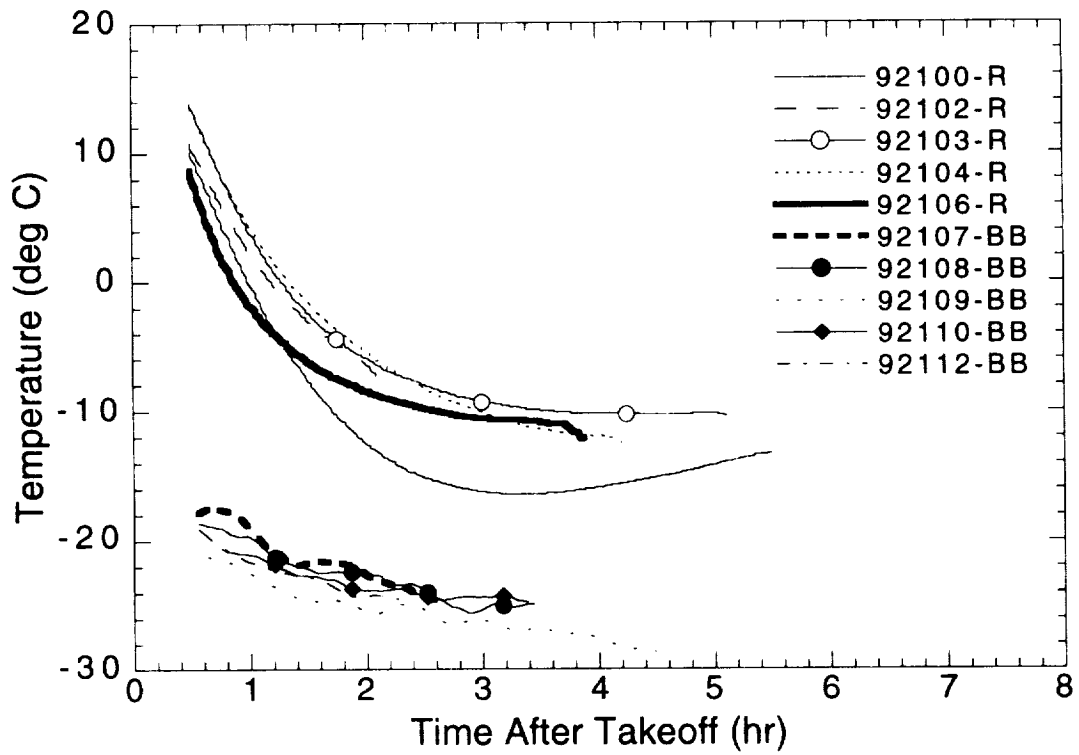


Figure 2. Rustrak (R) and ambient blackbody temperature (BB) data for ASTEX. Flights are listed by sortie number.

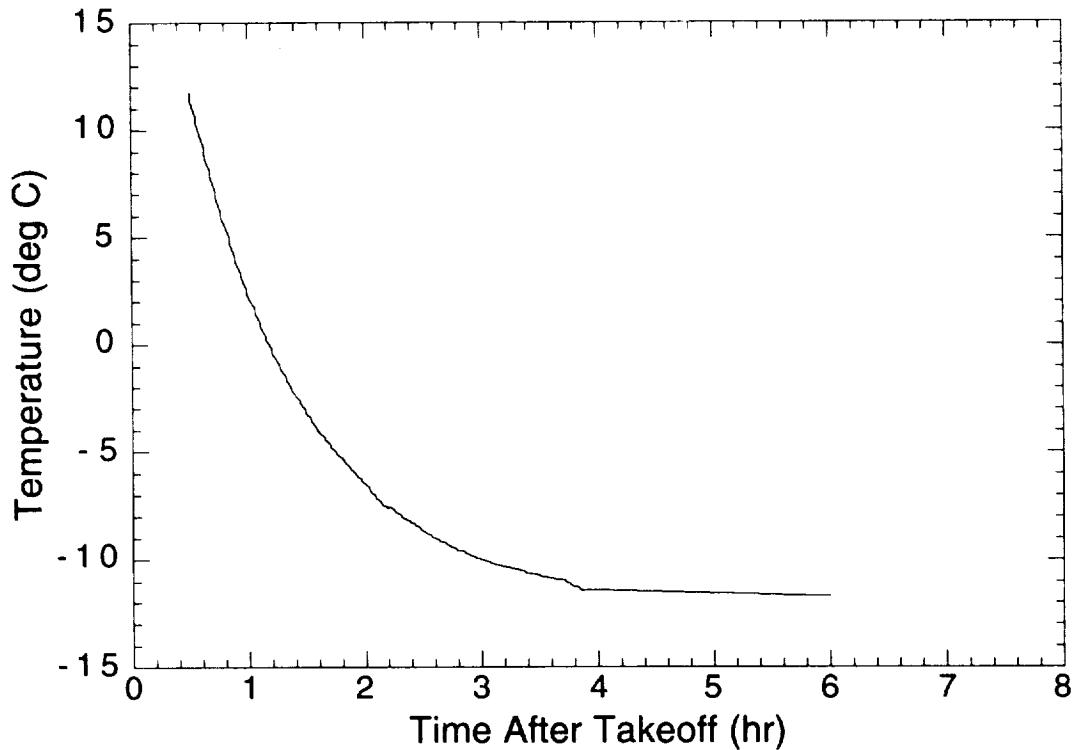


Figure 3. Average curve for ASTEX Rustrak temperature data, extrapolated to 6 hours after takeoff

Note that this expression is valid only from 0.5 to about 6 hours after takeoff (data are not typically recorded until after about 0.5 hr into a flight and no MAS ASTEX flights exceeded 6 hours).

Using  $T_{mas}$  as described above, expressions to characterize the change in calibration with temperature for each temperature sensitive channel are derived. These expressions in effect convert the in-flight earth-view counts to what that value would be if the measurement were taken at laboratory (+25°C) conditions. Thereby making the calibration coefficients from Table 6 applicable to the in-flight data. According to the data in Table 7 for ASTEX data only channels 5 and 6 are temperature sensitive. Also since there are only 2 data points the data are assumed to be linear, simplifying the equations. Using then for ASTEX an average of the pre- and post-flight chamber data, the following equations have been derived to adjust the in-flight earth-view counts values of channels 5 and 6:

Channel 5:

$$C_{lab} = (C_0 * g) + (C_{infl} - (C_0 * g)) / (0.0025 T_{mas} + 0.9382), \quad \text{where,} \quad (2)$$

- $C_{lab}$  - the effective counts value at laboratory conditions (+25°C), the counts value to actually apply the calibration coefficients to
- $C_{infl}$  - the recorded in-flight (earth-view) counts value
- $T_{mas}$  - the MAS instrument temperature (°C)
- $C_0$  - offset counts (number of counts recorded when observing cold blackbody) - note MAS data system always records  $C_0$  at a gain setting of 1.0. Also it is recommend that a running average of about 30 scans be used to smooth the  $C_0$  values
- $g$  - gain setting for  $C_{infl}$  (necessary to convert  $C_0$  to the same gain as  $C_{infl}$ )

Channel 6:

$$C_{lab} = (C_0 * g) + (C_{infl} - (C_0 * g)) / (0.0023 T_{mas} + 0.9436) \quad (3)$$

Some caution is necessary in the use of the above equations, since in the chamber tests, flight conditions are only partially simulated. Cooling rates of any temperature sensitive components might be quite different in the chamber as compared to in the aircraft pod. Also in the chamber the pressure is not reduced and therefore no effects due to the low pressure can be simulated. Furthermore the two above tests are based on only two data points and an estimated linear change. More testing in the chamber is necessary to determine more accurately the calibration change at temperatures between 25 and -35 °C.

## V. Intercomparison of Field Calibration to Ames 30-Inch Sphere Calibration

Before and after deployment, the MAS visible and near-infrared channels are calibrated at Ames using a 30-inch integrating sphere. Using this data, for every MAS flight, a calibration summary is produced and distributed to the principle investigator and archived in the flight files. In this summary the radiance/count values at gain of 1 are divided by the actual gain settings used on the specific data flight to yield the appropriate coefficients for that mission. When changes in the instrument occur during deployments affecting system performance, comments documenting these changes accompany the documentation.

To calibrate the MAS, the instrument is placed directly over the sphere either in the Ames lab or while mounted in the plane. No mirror is necessary. With six lamps illuminated in the sphere, data is recorded and digital counts are noted. The mean of the nadir point provides the digital counts that are incorporated with the sphere radiance, lamp intensity, offset value

(recorded observation of blackbody #1) and bandpass curves to produce a calibration coefficient of radiance/count at a gain of one. Radiance/count at a gain of 1 is calculated by equation 4 below.

$$L_{cg1} = (L_i * I_{nl}) / ((C_s - (C_0 * g_s)) / g_s), \quad \text{where,} \quad (4)$$

- $L_{cg1}$  = radiance per count @ gain = 1 (slope of counts to radiance conversion)
- $L_i$  = in-band sphere radiance with all six lamps illuminated, calculated by integrating the sphere radiance data over the MAS spectral bandpass (sphere radiance for peak wavelength in bandpass when full bandpass filter function is unavailable)
- $I_{nl}$  = adjustment factor for the number of lamps used during the calibration run (measured empirically by Optronic Labs)
- $C_s$  = raw counts viewing sphere
- $C_0$  = offset counts or tare value, taken while viewing blackbody #1  
The MAS data system always records this value at a gain of 1
- $g_s$  = gain setting used while viewing the sphere

The Ames 30-inch sphere, which has been in use since 1987, is calibrated by Optronic Laboratories Inc. on nearly an annual basis. Optronic determines the near normal spectral radiance of the exit aperture over the wavelength range of 350 to 2400 nm. Measurements are made at 10 nm intervals in the visible near-IR region, and at 20 nm interval in the IR. Three measurements are made; one with lamps 1, 2, 5, 6, 9, and 10 operating, one with lamps 3, 4, 7, 8, 11, and 12 operating, and lamp intensity values of one through twelve lamps. During most calibration runs, only six of the twelve lamps in the sphere are utilized at one time because the brightness exceeds most instruments tolerances. There is an average variance between these sets of lamps of only 0.9 percent. Overall, with five measurements since 1988 there has been an average of only 6 % variance between the yearly measurements. The radiance values for the Ames sphere for the ASTEX deployment are listed in Table 8. Since the sphere was relamped in July of 1992 (before post-deployment calibration), two sets of numbers are given in Table 8 for the sphere radiance. The 2/6/91 data applies to pre-deployment ASTEX calibration and the 7/14/92 data to the post-deployment ASTEX data.

Ames personnel use (when available) the bandpass integrated sphere radiance for term  $L_i$  in eqn. 4 when determining the calibration coefficients for each MAS channel. These values are given in Table 9. The MAS calibration using the Goddard hemisphere (section III of this report) however used the interpolated hemisphere radiance at the wavelength of maximum spectral response (peak response for each bandpass filter function - see Figures 10-14 for the shape of each spectral response curve). To compare the two methods of determining the appropriate sphere radiance for each MAS channel, Table 9 also lists the sphere radiance at the peak spectral response wavelength of each MAS channel. The two methods show only very small differences and thus either method is considered acceptable (the difference for the 2.14 $\mu$ m channel is slightly larger than the others but is still smaller than other error sources in the calibration at this wavelength).

Using the integrated 30-inch sphere radiance values for MAS channels 2-6 and the other appropriate information for equation 4, radiance/count factors were determined for each channel. Table 10 summarizes the results for the pre and post-deployment.

Table 8. Radiance Values for the Ames 30-Inch Sphere as Measured on 2/6/91 (for Pre-Deployment) and 7/14/92 (for Post-Deployment) With Lamps 1, 2, 5, 6, 9, 10 Illuminated.

Wavelength ( $\mu\text{m}$ )	Ames Sphere 2/6/91	Ames Sphere 7/14/92
0.50	77.0	72.4
0.55	116.0	110.6
0.60	157.1	150.1
0.65	195.7	186.7
0.70	229.3	218.7
0.75	251.2	242.6
0.80	269.8	260.4
0.85	282.2	268.9
0.90	287.8	270.2
0.95	281.4	266.3
1.00	273.1	260.5
1.05	263.6	253.8
1.10	252.4	244.2
1.15	236.4	228.7
1.20	219.3	212.6
1.25	207.2	201.8
1.30	195.2	190.5
1.35	170.3	165.4
1.40	147.0	143.2
1.45	122.6	119.2
1.50	120.2	116.4
1.55	115.7	112.7
1.60	107.4	104.6
1.65	101.5	98.8
1.70	95.2	93.2
1.75	82.8	81.8
1.80	72.1	70.0
1.85	64.2	62.0
1.90	45.6	44.0
1.95	37.6	36.7
2.00	42.0	41.0
2.05	40.5	39.6
2.10	35.0	34.3
2.15	36.1	34.1
2.20	30.8	28.6

Table 9. MAS Radiance for Each Channel Calculated Both from the Bandpass Peak Power Point, and Integrated (Weighted) Over the Bandpass Filter (Pre-Deployment - 2/6/91, and Post-Deployment - 7/14/92).

MAS Peak Power Wavelength ( $\mu\text{m}$ )	Radiance at Peak Power Point (Pre-Deployment)	Radiance Integrated w/bandpass (Pre-Deployment)	Radiance at Peak Power Point (Post-Deployment)	Radiance Integrated w/bandpass (Post-Deployment)
0.664	20.60	20.27	19.73	19.37
0.875	28.76	28.52	26.95	26.97
0.945	28.21	28.17	26.69	26.63
1.623	10.47	10.49	10.18	10.21
2.142	3.72	3.58	3.51	3.38

Note radiance units are  $\text{W m}^{-2} \mu\text{m}^{-1} \text{sr}^{-1}$ .

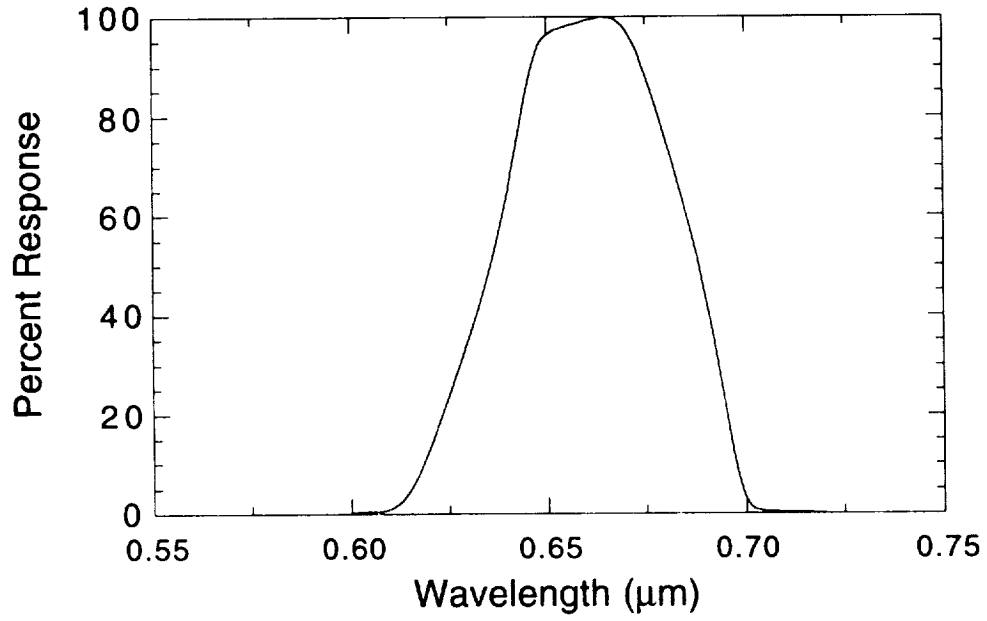


Figure 10. MAS channel 2 spectral bandpass filter. Peak power point is at 0.664 μm.

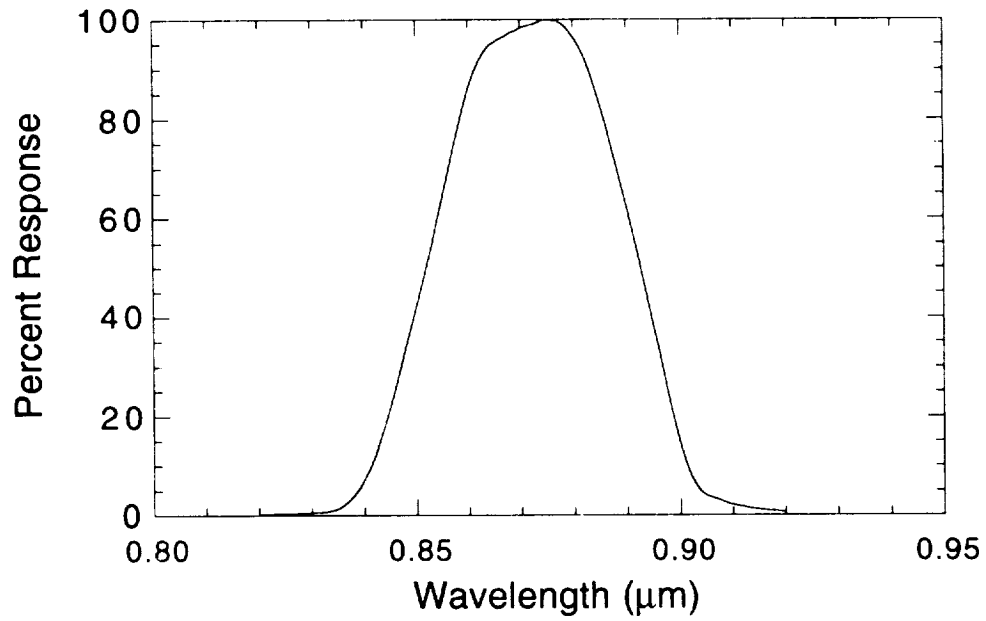


Figure 11. MAS channel 3 spectral bandpass filter. Peak power point is at 0.875 μm.

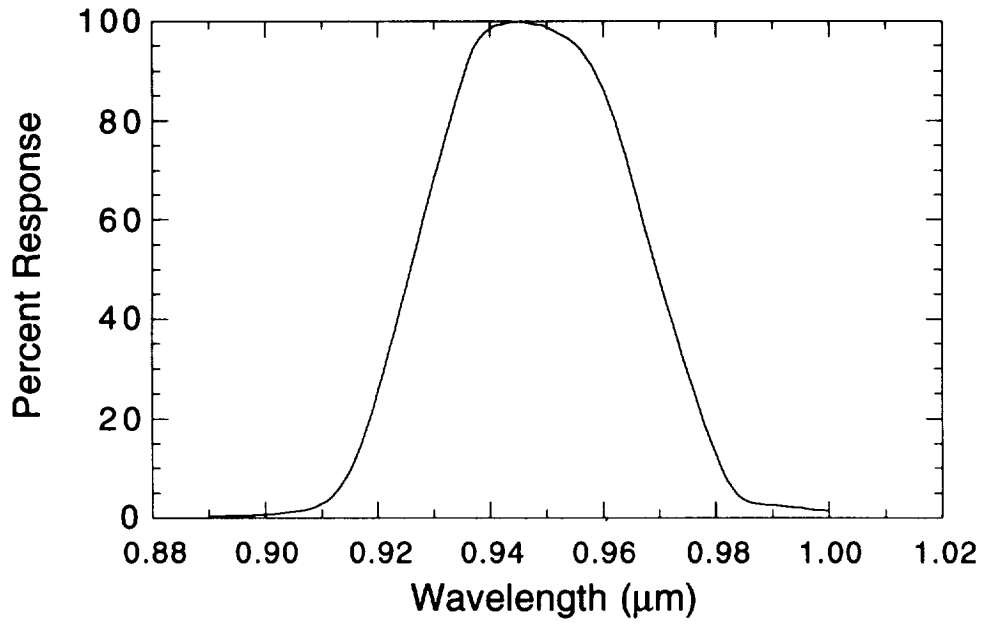


Figure 12. MAS channel 4 spectral bandpass filter. Peak power point is at 0.945 μm.

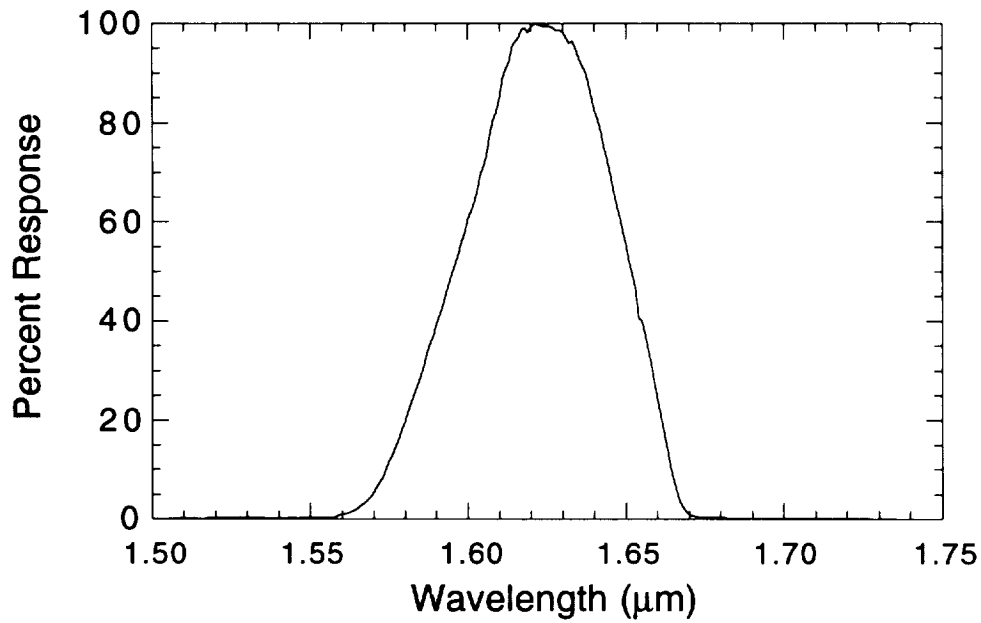


Figure 13. MAS channel 5 spectral bandpass filter. Peak power point is at 1.623 μm.

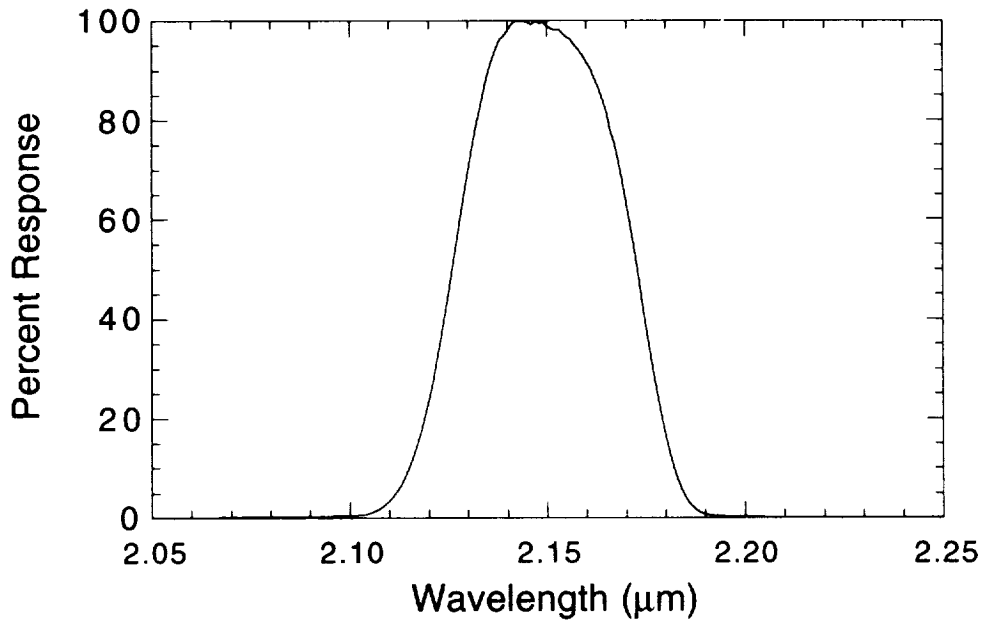


Figure 14. MAS channel 6 spectral bandpass filter. Peak power point is at 2.142  $\mu\text{m}$ .

Table 10. Ames Pre and Post FIRE-Cirrus Radiance/Count Values and Their Ratio

Channel	Wavelength ( $\mu\text{m}$ )	Ames pre-ASTEX	Ames post-ASTEX	Ratio Post/Pre
2	0.665	0.1325	0.3588	2.708
3	0.875	0.1828	0.2192	1.199
4	0.945	0.1214	0.1221	1.006
5	1.623	0.0481	0.0510	1.060
6	2.142	0.0442	0.0457	1.034

The substantial difference in channels 2 and 3 is largely due to the resistor changes made during the deployment. The resistor changes were necessary due to a saturation condition in the MAS electronics that ‘clipped’ the counts at a value less than the maximum possible value of 255 counts. According to the types of the resistors installed, the radiance/count values for channels 2 and 3 for the Ames pre-ASTEX data should change by about 380% and 100% respectively. This would increase the radiance/count values of 0.1325 and 0.1828 in Table 10 to values of 0.636 and 0.3756. Compared to the Ames post-ASTEX data these values are considerably larger. However inspection of the raw counts for the Ames pre-ASTEX calibration data suggests that the ‘clipping’ affected the calibration. The counts values for channels 2 and 3 of 158 and 160, observed at the 6 lamp setting of the sphere, match the counts at which analysis of the flight data shows clipping. Thus it is likely the counts value that would have been recorded had there been no clipping would have been some unknown amount higher. Increasing the counts values above the recorded values of 158 and 160 would have the effect of lowering the radiance/count values (from the 0.635 and 0.3756 values). As a result of this uncertainty, the radiance/count values in Table 10 for pre-ASTEX channel 2 and 3 data are not considered valid. Furthermore inspection of the raw counts for channel 4 suggests a similar problem. Observations of the flight data shows that channel 4 was clipping at 236 counts, which corresponds to the recorded counts value (at 6

lamps) observed in Ames calibration. In this case, both pre- and post-ASTEX radiance/count values are invalid since no attempt was made to correct the clipping problem in channel 4 during the deployment.

To compare the Goddard hemisphere calibration values (from Table 6 (a-d)), to the Ames results, an average was taken of the pre- and post-ASTEX Ames data (using only the valid radiance/count values). The resulting average calibration values for the Ames data are compared to the hemisphere derived values in Table 10 below.

Table 11. Comparison of the Hemisphere Radiance/Count values for ASTEX Data With the Average of Ames Pre and Post ASTEX Radiance/Count Values

Channel	Wavelength	AMES Avg	Hemisphere	Hemi/Ames
2	0.6650	0.3588	0.3741	1.043
3	0.8750	0.2192	0.2392	1.091
4	0.9450		0.6755	
5	1.6230	0.04955	0.0514	1.037
6	2.1420	0.04495	0.0430	0.956

Generally the agreement is quite good. Disagreement in channel 3 is more than the others but possibly this is due to humidity differences between the calibrations. The good agreement is encouraging given the difference in the calibrations, i.e., two different calibration sources (calibrated by two different groups), use of 45° inclined front surface mirror for one of the calibrations, and the use of the spectral response curves by Ames personnel in their calibration analysis (rather than just using the central wavelength as in the hemisphere calibration analysis).

## VI. Future Calibration Work

All future light source calibrations (beginning in 1994) will be conducted every 0.01  $\mu\text{m}$ . Also rather than using just the radiance at the peak spectral response (as in section III), the source radiance value for each MAS channel will routinely be determined by integration over the appropriate spectral bandpass of each MAS channel. In addition future publications will describe in much greater detail possible error sources in the calibration, and also a report will be issued on the results of laboratory tests (conducted at Ames) of spectral noise (shifting) for each MAS channel.

REPORT DOCUMENTATION PAGE			Form Approved OMB No. 0704-0188	
Public reporting burden for this collection of information is estimated to average 1 hour per response, including the time for reviewing instructions, searching existing data sources, gathering and maintaining the data needed, and completing and reviewing the collection of information. Send comments regarding this burden estimate or any other aspect of this collection of information, including suggestions for reducing this burden, to Washington Headquarters Services, Directorate for Information Operations and Reports, 1215 Jefferson Davis Highway, Suite 1204, Arlington, VA 22202-4302, and to the Office of Management and Budget, Paperwork Reduction Project (0704-0188), Washington, DC 20503.				
1. AGENCY USE ONLY (Leave blank)	2. REPORT DATE March 1994	3. REPORT TYPE AND DATES COVERED Technical Memorandum		
4. TITLE AND SUBTITLE MODIS Airborne Simulator Visible and Near-Infrared Calibration - 1992 ASTEX Field Experiment <i>Calibration Version - ASTEX King 1.0</i>			5. FUNDING NUMBERS  913	
6. AUTHOR(S) G. Thomas Arnold, Michael Fitzgerald, Patrick S. Grant, and Michael D. King				
7. PERFORMING ORGANIZATION NAME(S) AND ADDRESS (ES)  Goddard Space Flight Center Greenbelt, Maryland 20771			8. PERFORMING ORGANIZATION REPORT NUMBER  94B00055	
9. SPONSORING / MONITORING AGENCY NAME(S) AND ADDRESS (ES)  National Aeronautics and Space Administration Washington, DC 20546-0001			10. SPONSORING / MONITORING AGENCY REPORT NUMBER  NASA TM-104599	
11. SUPPLEMENTARY NOTES Arnold: Applied Research Corporation, Landover, Maryland; Fitzgerald and Grant: ATAC, Mountain View, California; King: Goddard Space Flight Center, Greenbelt, Maryland				
12a. DISTRIBUTION / AVAILABILITY STATMENT  Unclassified - Unlimited Subject Category 47			12b. DISTRIBUTION CODE	
13. ABSTRACT (Maximum 200 words) Calibration of the visible and near-infrared channels of the MODIS Airborne Simulator (MAS) is derived from observations of a calibrated light source. For the 1992 ASTEX field experiment, the calibrated light source was the NASA Goddard 48-inch integrating hemisphere. Laboratory tests during the ASTEX field experiment were conducted to calibrate the hemisphere and from the hemisphere to the MAS. The purpose of this report is to summarize the ASTEX hemisphere calibration, and then describe how the MAS was calibrated from observations of the hemisphere data. All MAS calibration measurements are presented, and determination of the MAS calibration coefficients (raw counts to radiance conversion) is discussed. Thermal sensitivity of the MAS visible and near-infrared calibration is also discussed. Typically, the MAS in-flight is 30 to 60 degrees C colder than the room temperature laboratory calibration. Results from in-flight temperature measurements and tests of the MAS in a cold chamber are given, and from these, equations are derived to adjust the MAS in-flight data to what the value would be at laboratory conditions. For ASTEX data, only channels 5 and 6 were found to be temperature sensitive. The final section of this report describes comparisons to an independent MAS laboratory calibration by Ames personnel using their 30-inch integrating sphere.				
14. SUBJECT TERMS Calibration - radiometric, remote sensing - instrumentation, MODIS, MODIS Airborne Simulator, ASTEX, FIRE-cirrus			15. NUMBER OF PAGES 28	
			16. PRICE CODE	
17. SECURITY CLASSIFICATION OF REPORT Unclassified	18. SECURITY CLASSIFICATION OF THIS PAGE Unclassified	19. SECURITY CLASSIFICATION OF ABSTRACT Unclassified	20. LIMITATION OF ABSTRACT UL	